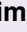






Genome-Enabled Analysis of Population Dynamics and Virulence-Associated Loci in the Oat Crown Rust Fungus *Puccinia coronata* f. sp. *avenae*

Tim C. Hewitt,¹  Eva C. Henningsen,¹  Danilo Pereira,^{2,3} Kerensa McElroy,¹ Eric S. Nazareno,⁴ Sheshanka Dugyala,⁴ Hoa Nguyen-Phuc,⁴ Feng Li,⁴  Marisa E. Miller,⁴ Botma Visser,⁵ Zacharias A. Pretorius,⁵ Willem H. P. Boshoff,⁵ Jana Sperschneider,¹  Eva H. Stukenbrock,^{2,3} Shahryar F. Kianian,^{4,6} Peter N. Dodds,¹  and Melania Figueroa^{1,†}

¹ Commonwealth Scientific and Industrial Research Organisation, Agriculture and Food, Canberra, ACT 2600, Australia

² Christian Albrechts University of Kiel, 24118 Kiel, Germany

³ Max Planck Institute of Evolutionary Biology, 24306 Plön, Germany

⁴ Department of Plant Pathology, University of Minnesota, St. Paul, MN 55108, U.S.A.

⁵ Department of Plant Sciences, University of the Free State, Bloemfontein 9300, South Africa

⁶ USDA-ARS Cereal Disease Laboratory, St. Paul, MN 55108, U.S.A.

Accepted for publication 9 November 2023.

Puccinia coronata f. sp. *avenae* (*Pca*) is an important fungal pathogen causing crown rust that impacts oat production worldwide. Genetic resistance for crop protection against *Pca* is often overcome by the rapid virulence evolution of the pathogen. This study investigated the factors shaping adaptive evolution

of *Pca* using pathogen populations from distinct geographic regions within the United States and South Africa. Phenotypic and genome-wide sequencing data of these diverse *Pca* collections, including 217 isolates, uncovered phylogenetic relationships and established distinct genetic composition between populations from northern and southern regions from the United States and South Africa. The population dynamics of *Pca* involve a bidirectional movement of inoculum between northern and southern regions of the United States and contributions from clonality and sexuality. The population from South Africa is solely clonal. A genome-wide association study (GWAS) employing a haplotype-resolved *Pca* reference genome was used to define 11 virulence-associated loci corresponding to 25 oat differential lines. These regions were screened to determine candidate *Avr* effector genes. Overall, the GWAS results allowed us to identify the underlying genetic factors controlling pathogen recognition in an oat differential set used in the United States to assign pathogen races (pathotypes). Key GWAS findings support complex genetic interactions in several oat lines, suggesting allelism among resistance genes or redundancy of genes included in the differential set, multiple resistance genes recognizing genetically linked *Avr* effector genes, or potentially epistatic relationships. A careful evaluation of the composition of the oat differential set accompanied by the development or implementation of molecular markers is recommended.

†Corresponding author: M. Figueroa; melania.figueroa@csiro.au

Current address for F. Li: eGenesis, 101 Cambridge Park Drive, Cambridge, MA 02140, U.S.A.

Current address for M. E. Miller: Pairwise Plants, LLC, Durham, NC, U.S.A.

Current address for H. Nguyen-Phuc: Department of Molecular Virology and Microbiology, Baylor College of Medicine, Houston, TX 77030, U.S.A.

Author contributions: T.C.H.: phylogenetic analysis, variant analysis, GWAS, interpretation, and original drafting of the article; D.P.: population structure, LD decay, and selective sweep analysis; E.C.H.: rust infections of U.S. *Pca* populations, race assignments, DNA extractions, and data visualization; K.M.: data curation and GWAS methodology; E.S.N., S.D., H.N.-P., and F.L.: U.S. rust collections and infections; M.E.M.: U.S. rust collections; B.V., Z.A.P., and W.H.P.B.: South Africa rust resources, curation, and race assignments; J.S.: supervision, effector prediction, and drafting of the article; E.H.S.: conceptualization and methodology; S.F.K.: conceptualization and U.S. rust collection; P.N.D., conceptualization, original drafting of the article, and supervision; M.F.: conceptualization, project administration, supervision, original drafting of the article, U.S. rust collection and infections. All authors contributed to editing and review of the article.

Funding: Data used in this project were acquired through a USDA National Institute of Food and Agriculture grant award (2018-67013-27819) to M. Figueroa, a USDA National Institute of Food and Agriculture Postdoctoral Fellowship Award (2017-67012-26117) to M. E. Miller, and funding from PepsiCo, Inc. T. C. Hewitt is supported by a Commonwealth Scientific and Industrial Research Organisation (CSIRO) Research Office Postdoctoral Fellowship.

e-Xtra: Supplementary material is available online.

The author(s) declare no conflict of interest.



Copyright © 2024 The Author(s). This is an open access article distributed under the CC BY-NC-ND 4.0 International license.

Keywords: disease, effector, genetic variation, oat, rust, virulence

Puccinia coronata f. sp. *avenae* (*Pca*) is an important foliar pathogen that causes oat crown rust, which impacts oat production around the world (Nazareno et al. 2018). An effective method to control rust diseases is the use of genetic resistance in crops through the incorporation of resistance (*R*) genes (Ellis et al. 2014). Most *R* genes encode immune receptors that can recognize specific secreted proteins from the pathogen, known as avirulence (*Avr*) effectors (Dodds 2023; Dodds and Rathjen 2010). Such a recognition event is essential to mount an immune response that prevents the pathogen's growth in the plant. Despite the potential benefits of genetic resistance in agriculture, the use of *R* genes to manage *Pca* infections in the field

has not been as effective as needed, given that most released oat *R* genes have shown limited durability against crown rust (Figueroa et al. 2020; Nazareno et al. 2018). Sexual recombination, random (sequential) mutation, and somatic hybridization are some of mechanisms that allow rust pathogens such as *Pca* to alter their genetic makeup and gain virulence in otherwise resistant cultivars (Duplessis et al. 2021; Figueroa et al. 2020; Möller and Stukenbrock 2017).

Pca shares a similar life cycle with other *Puccinia* species that infect cereals. This involves alternation between an asexual cereal infection phase mediated by dikaryotic urediniospores (containing two different haploid nuclei), and a sexual phase that occurs on an alternate host. Thus, populations of cereal rust fungi can be highly sexual when the alternate host is present, but in its absence, the asexual phase can persist indefinitely, giving rise to long-lived clonal populations (Figueroa et al. 2020). For instance, populations of wheat stem and leaf rust fungi (*Puccinia graminis* f. sp. *tritici* [*Pgt*] and *Puccinia triticina* [*Pt*], respectively) are predominately clonal because of the absence of the alternate sexual hosts (*Berberis* spp. and *Thalictrum* spp., respectively) in most parts of the world (Bolton et al. 2008; Patpour et al. 2022; Saunders et al. 2019). For oat crown rust, in countries such as South Africa where the alternate host buckthorn (*Rhamnus* spp.) is absent, reproduction is completely asexual. In areas such as the northern United States, the oat crown rust fungus is capable of both sexual and asexual (clonal) reproduction because of the wide prevalence of common buckthorn (*Rhamnus cathartica*), which permits the sexual life cycle to occur on a seasonal basis (Nazareno et al. 2018). However, buckthorn is absent from southern U.S. oat-growing regions where asexual reproduction is predicted to play a major role (Rawlins et al. 2018). In some geographic regions, the epidemiology of *Pca* is also impacted by the presence of wild oats near cropping fields, which can also facilitate asexual reproduction. Ongoing race surveys in the United States have found an extreme diversity of virulence phenotypes in the *Pca* population (Carson 2011). The Rust Surveillance Annual Surveys assign race pathotypes to *Pca* isolates based on infection phenotypes on the North American oat differential set using 4-letter and 10-letter codes corresponding to virulence scores on 16 and 40 oat differential lines respectively (Chong et al. 2000). For example, between 2006 and 2009, 201 races were found among the 357 isolates from the spring oat region of the north-central United States, and 140 races were found among 214 isolates from the southern winter oat region (Carson 2011).

More than 100 *R* genes against oat crown rust (commonly designated as *Pc* genes) have been postulated (Nazareno et al. 2018). However, no *Pc* gene has yet been cloned, and the limited molecular and genetic data for most resistance sources make it difficult to assess whether they contain unique *Pc* genes or combinations of several *Pc* genes. The complex rearrangements observed between the sequenced oat genomes (Kamal et al. 2022; Peng et al. 2022; PepsiCo 2021) mean that orthologous *Pc* genes may not always occur in the same location, compounding the difficulties in assigning unique *Pc* gene designations. Consequently, the limited durability of introduced *Pc* genes in the field may be partially caused by reintroduction of preexisting genes or their allelic variants in breeding programs. Members of differential sets to complete race assignments are often selected to represent unique *R* genes; however, in the absence of genetic characterization and molecular data of *Pc* genes, it has been noted that various members of oat differential sets could include the same *Pc* gene or its alleles (Miller et al. 2020). No *Avr* genes have yet been isolated from *Pca*. Until recently, the complex dikaryotic genomes of rust fungi have hampered genetic analyses of virulence genes, with the only *Avr* effectors isolated from cereal rusts so far being from the wheat stem rust pathogen (*P. graminis* f. sp. *tritici*) using

mutational and high-throughput screening approaches (Arndell et al. 2023; Chen et al. 2017; Salcedo et al. 2017; Upadhyaya et al. 2021). Genome-wide association studies (GWAS) are emerging as a powerful approach to identify *Avr* loci in plant pathogens (Gao et al. 2016; Kariyawasam et al. 2022; Kloppe et al. 2023; Martin et al. 2020; Zhong et al. 2017), but require highly complete genome references and population data from sexually reproducing populations. Advances in sequencing technologies and computational pipelines for haplotype phasing (Duan et al. 2022; Li et al. 2019; Sperschneider et al. 2022) have created new opportunities for applying such genome-wide approaches. Miller et al. (2018) generated the first partially haplotype-separated genome references for two *Pca* isolates, 12SD80 and 12NC29. These resources facilitated a population genomics study of a limited set of U.S. *Pca* isolates from 1990 and 2015 that found a significant shift in population genetics and virulence over this time (Miller et al. 2020). A GWAS of this population also identified 7 genomic regions associated with avirulence phenotypes on 15 *Pc* genes, and indicated for the first time that different *Pc* genes may detect *Avr* genes at the same or closely linked loci. However, the 12SD80 and 12NC29 genome assemblies are quite fragmented, and many of the *Pc* genes elicited association peaks across multiple assembled contigs whose relative positions in the *Pca* genome were not clear. We recently developed a complete chromosome-level and nuclear-phased reference genome of *Pca* (Pca203) (Henningesen et al. 2022), and we use this resource here to expand on the initial findings reported by Miller et al. (2020) through analysis of a much larger population of U.S. *Pca* isolates. This reveals a primary role for local sexual reproduction in the northern U.S. population and extensive migration between southern and northern regions. Inclusion of isolates from South Africa allowed us to investigate pathotype diversity in the absence of the sexual phase, demonstrating likely single-mutation events leading to multiple virulence gains. Our GWAS, using a larger *Pca* set with the Pca203 genome reference, identified a total of 11 virulence-associated genomic intervals (VGIs) associated with virulence phenotypes on 25 oat differential lines postulated to carry different *Pc* genes. Multiple oat lines have several corresponding VGIs, suggesting the presence of multiple *Pc* genes, many of which overlap between different oat differential lines. These results allowed us to identify *Avr* effector candidates from these regions for future testing and validation and may also expedite the isolation of *Pc* genes in the host.

Results

Pca populations exhibit increased virulence in geographic regions where the sexual host is present

To assess pathotype (race) variation in the U.S. *Pca* population, we compared virulence scores for 185 isolates on the set of 40 oat resistance differential lines routinely used in the United States (Chong et al. 2000; Nazareno et al. 2018; Supplementary Data S1). These include 30 isolates collected in 1990 and 30 from 2015 that were previously characterized (Miller et al. 2020); the three reference isolates Pca203, 12SD80, and 12NC29 (Henningesen et al. 2022; Miller et al. 2018); and an additional 122 isolates collected from 2015 to 2018. Of this total set, 93 isolates were sampled from the Minnesota Matt Moore Buckthorn Nursery either as aeciospores directly from buckthorn plants (46 isolates) or as urediniospores from oats growing in the nursery and infected from the adjacent buckthorn sources (47 isolates). A total of 147 unique races were detected out of 185 isolates.

To assess recent regional diversity of *Pca*, we focused on isolates collected from 2015 to 2018, because a substantial virulence shift was documented post-1990 (Miller et al. 2020). Consistent with their recent sexual recombination history, all buckthorn nursery isolates had a unique race. Field-derived

isolates were also highly diverse, with 65 races detected among 69 isolates. However, the buckthorn nursery isolates showed a significantly higher frequency of virulence phenotypes compared with field isolates ($P = 6.795 \times 10^{-10}$, Wilcoxon rank sum test) (Fig. 1A and B). Among the field-derived samples, pathotype diversity was similarly high in northern states with prevalent buckthorn (30 races/31 isolates) and southern states where buckthorn is rare or absent (25 races/26 isolates). However, there was also a higher frequency of virulence phenotypes in the northern versus southern states ($P = 1.673 \times 10^{-6}$, Wilcoxon rank sum test) (Supplementary Fig. S1A and B). We also observed differences in virulence distributions on individual oat differential lines between these populations. Nursery-derived isolates showed significantly higher virulence scores ($P < 0.01$, Wilcoxon rank sum test) compared with field isolates on the differential lines Pc91, 'HiFi', Pc48, Pc52, Pc68, Pc53, Pc50, 'Stainless', 'Belle', 'TAM-O-405', Pc96, Pc94, and 'Leggett' (Fig. 1C). The nursery-derived isolates displayed lower virulence on the lines Pc55, Pc38, Pc56, Pc39, Pc67, and Pc63 compared with field-derived isolates. Similarly, the northern isolates showed higher virulence ($P < 0.01$, Wilcoxon rank sum test) compared with southern isolates on Pc91, HiFi, Pc48, Pc52, Pc68, Pc50, Pc63, Pc45, and IAB605Xsel lines (Supplementary Fig. S1C). In addition to these regional differences, changes were noted between the years 2015 and 2017 in field-derived isolates. Specifically, virulence frequencies

on Pc68, Pc91, and HiFi differential lines (score ≥ 7) rose from 26 to 30% in 2015 to 43 to 46% in 2017 (Supplementary Fig. S1A).

In contrast to the U.S. *Pca* population, we only recorded six different races in a set of 32 *Pca* isolates from South Africa (Boshoff et al. 2020; Supplementary Data S1; Supplementary Fig. S2). No virulence was recorded on differential lines Pc36, Pc50, Pc56, Pc60, Pc62, Pc64, Pc68, Pc91, Pc94, Pc96, Pc-H548, and Pc-WIX 1,2, for which virulence commonly occurs in the United States. This lower virulence prevalence and variation of South African isolates is consistent with the absence of buckthorn in this country limiting *Pca* to asexual reproduction, in addition to population size and genetic drift as potential contributors.

Structure and diversity of *Pca* populations varies between geographic regions

We generated Illumina whole-genome DNA sequencing data for all 154 new *Pca* isolates and combined this with existing sequence data for 63 isolates (Henningsen et al. 2022; Miller et al. 2018, 2020) to examine population genetic diversity. Reads were aligned to the 12SD80 reference assembly for variant calling. All samples showed a genome-wide average of at least 30× read coverage (Supplementary Fig. S3) with expected distributions of allelic frequencies (Supplementary Fig. S4). A neighbor-net network generated from 922,125 biallelic single-nucleotide

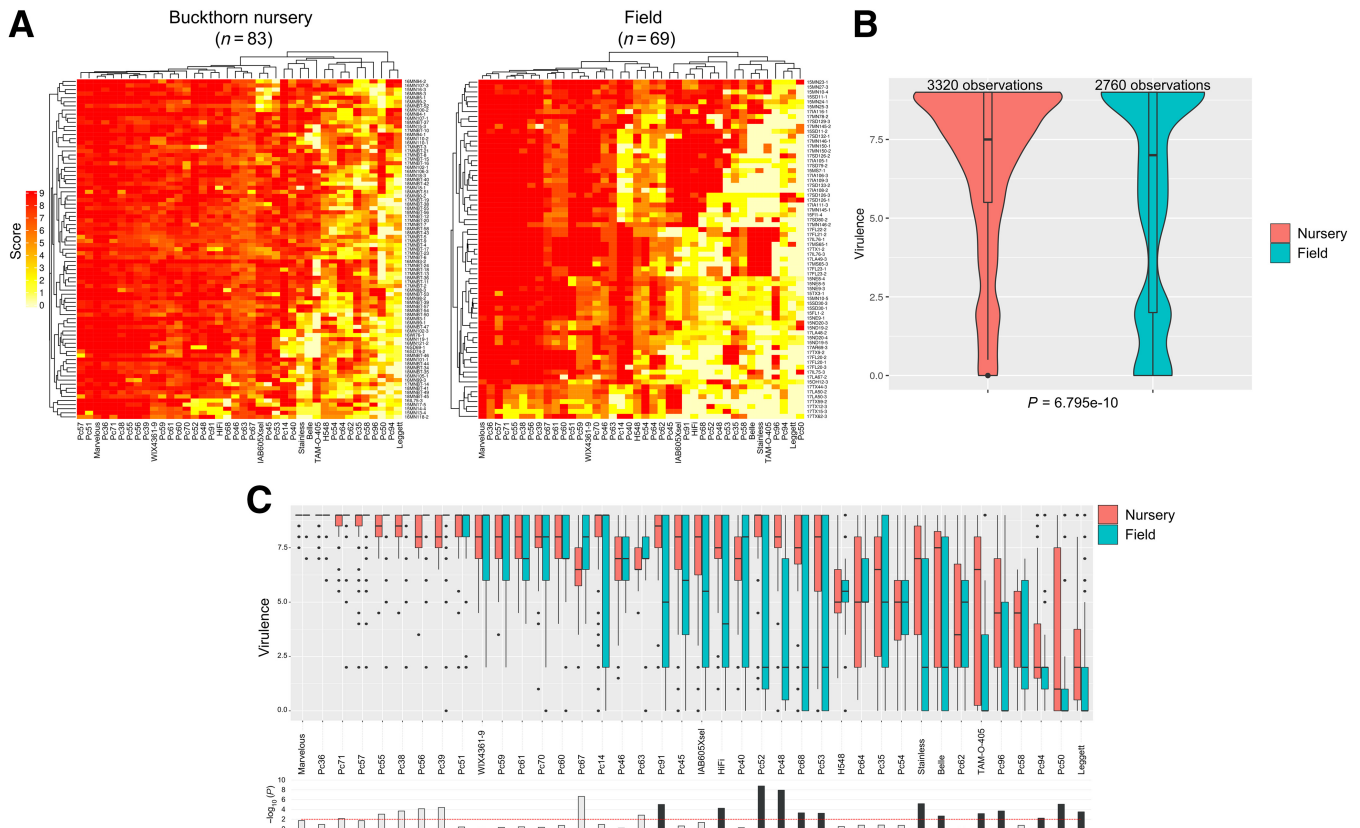


Fig. 1. Comparison of virulence profiles of *Puccinia coronata* f. sp. *avenae* (*Pca*) isolates from a buckthorn nursery and the field in the United States. **A**, Heat maps of virulence scores of *Pca* isolates (y axis) on 40 oat differential lines (x axis) comparing isolates from 2015 or later (excluding isolates from 1990). High infection scores (red) indicating high virulence, and lower scores (yellow/white) indicate avirulence. Order of *Pca* isolates is presented according to hierarchical clustering of virulence scores. **B**, Data shown in heat maps are summarized in violin plots, which depict distribution of all virulence scores for each group. The number of observations ($n = Pca$ isolate \times oat differential line [*Pc* gene]) is provided above each plot. A P value from a two-tailed Wilcoxon rank sum test is shown. **C**, Box plots of virulence scores on each differential line comparing nursery (red bars) versus field (teal bars). Black dots represent outliers. Plots ordered from highest to lowest mean virulence. Bottom panels display bar graphs of $-\log_{10}$ of P values from two-tailed Wilcoxon rank sum tests of difference between groups. The red dashed line indicates a significance threshold of $P = 0.01$. Bars with black fill mark differentials on which the virulence distribution is significantly higher in the nursery group.

polymorphisms (SNPs) (Supplementary Fig. S5) showed that the U.S. population is dominated by a large, unstructured reticulated grouping consistent with a history of sexual recombination. A pairwise homoplasmy index (PHI) test on this group strongly supported the contribution of recombination ($P < 10^{-12}$) to the diversity of the population. There was also a single distinct outgroup of U.S. isolates, mainly from 1990, that was divergent from the main group. The South African population formed another more divergent outgroup that was very tightly clustered, and a PHI test did not provide strong support for a contribution of recombination to genetic diversity ($P = 0.0464$). The three wild oat-derived isolates formed a separate cluster in this group. Interestingly, a single U.S. isolate collected from the buckthorn

nursery in 1990, 90MN5B-1, appears closely related to the South African population.

These overall relationships were also evident in a maximum-likelihood (ML) phylogenetic tree (Fig. 2), where the sexual recombination history in the U.S. population is reflected in the low bootstrap support values for most nodes, especially among northern and nursery-derived isolates. However, there are several clonal groups evident (A to E) that consist of isolates separated by extremely short branch lengths connected by nodes with high bootstrap values. These clonal lineages include mostly southern U.S.-derived isolates, consistent with absence of the sexual host in those regions (Miller et al. 2020). However, the presence of both northern and southern isolates in some of these

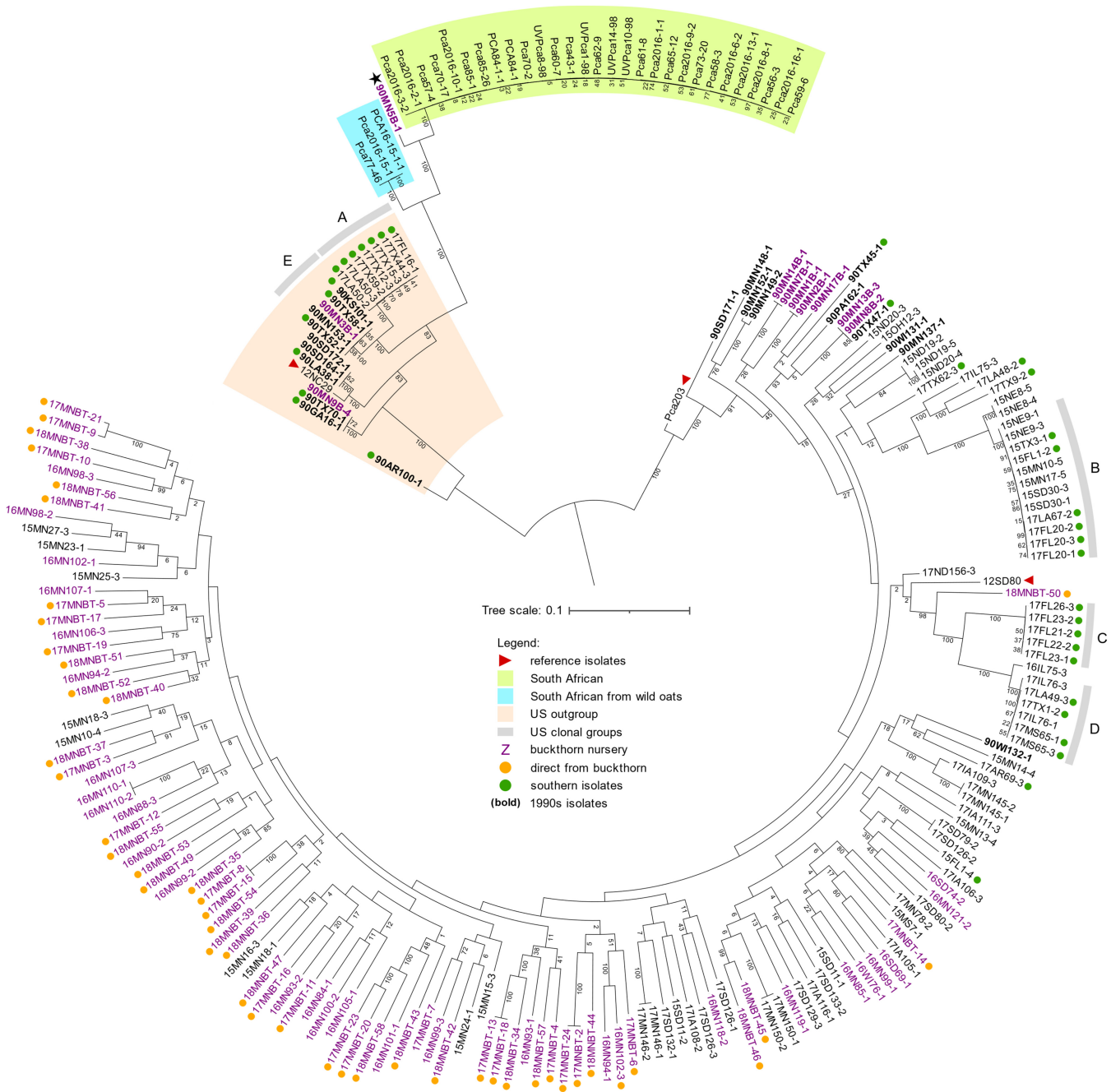


Fig. 2. Maximum-likelihood phylogenetic tree of *Puccinia coronata* f. sp. *avenae* (*Pca*) isolates from the United States and South Africa. The phylogeny is mid-rooted and based on 922,125 single-nucleotide polymorphism variants called against the 12SD80 genome reference with support values from 500 bootstraps shown below branches. Scale bar indicates nucleotide substitutions per site. Groups of interest are colored according to legend inset. Outlying U.S. isolate 90MN5B-1 is indicated with a black asterisk. Clonal groups with more than three members are labeled A to E.

clonal groups (B, D, and E) suggests migration of rust isolates between geographic regions. Again, the South African population is divergent from the U.S. population and falls into just two clonal groups, one consisting of the three isolates collected from wild oats and the other containing all 29 isolates from cultivated oat. The latter group comprises isolates collected between 1998 and 2018 from a broad geographic region, which is consistent with an asexual population dominated by a single clonal lineage in South Africa. As in the neighbor-net network, U.S. isolate 90MN5B-1 sits among the South African isolates in the phylogeny, suggesting it may be part of a globally dispersed lineage. Genotypic variation was very high in the greater U.S. population ($n = 165$), with variation at 821,833 out of 831,051 SNP sites, and the U.S. outgroup ($n = 20$), with variation at 652,504 out of 756,980 SNP sites. In contrast, only 47,369 out of 548,091 SNP sites were variable within the South African cultivated oat-derived population. Again, this is consistent with the contrasting clonal and sexual reproduction of these two populations.

To determine the population structure of the pathogen population, the SNP dataset was pruned for linkage disequilibrium (LD) using an r^2 cutoff of 0.6 to a set of 132,571 unlinked SNPs. A principal component analysis (Supplementary Fig. S6A) showed a clear differentiation of the cultivated oat-derived South African isolates from all other isolates, but no other clear groupings. Cluster membership analysis omitting isolates from 1990 was performed (Fig. 3A; Supplementary Fig. S6B and C), revealing that the nursery-derived isolates displayed a high degree of admixture, which is consistent with a history of sexual recombination. Some U.S. field-derived isolates showed single-cluster membership, consistent with the presence of asexually reproducing clonal groups, yet admixture is still evident in most isolates, especially those originating from northern regions. Most clusters are detected in both northern and southern U.S. *Pca* isolates, except for clusters 4 and 5, which comprise clonal groups A and C (Fig. 2), with each showing homogeneous cluster memberships. This supports the hypothesis that divergent lineages persist asex-

ually in the southern United States. The South African isolates from cultivated oats display no admixture and belong to a single cluster (1), while the three isolates from wild oats showed admixture between clusters 1 and 4, suggesting a relationship with the southern U.S. clonal group A. Overall, these population analyses all support that the U.S. *Pca* population is predominantly sexual, with some clonal lineages persisting over time, particularly in the southern regions, in contrast to the South African population, which is entirely clonal and consists of a single lineage.

Analysis of LD was performed using SNPs called on chromosome 1A of the *Pca*203 genome reference (Henningsen et al. 2022; Fig. 3B) to enable longer physical distance-based calculations. The highest rate of LD decay was shown in the U.S. population from the buckthorn nursery. The northern field population exhibited a similar rate of LD decay, consistent with a high frequency of sexual recombination in these populations caused by the presence of buckthorn. Conversely, the southern field population showed a notably lower rate of LD decay, consistent with a lack of local recombination in the absence of buckthorn, but with some LD decay maintained via migration occurring from regions with buckthorn. For the South African population, SNP sites were in complete disequilibrium, and no LD decay was detected, consistent with asexual reproduction.

Virulence phenotypes do not inform genetic relationships among diverse *Pca* isolates

Most rust surveillance programs rely heavily on pathotype (race) analysis using a limited set of host-resistant differential lines, but it is not always clear whether this provides sufficient discrimination between lineages. We compared the virulence profiles and genotypes of a subset of 65 U.S. isolates including representatives of diverse clonal groups. These data showed different groupings when clustered by virulence profile or by SNP phylogeny (Supplementary Fig. S7). While most clonally related *Pca* isolates showed near-matching virulence profiles, the reverse was not always true, as some isolates with highly similar virulence profiles belonged to genetically diverse groups. For

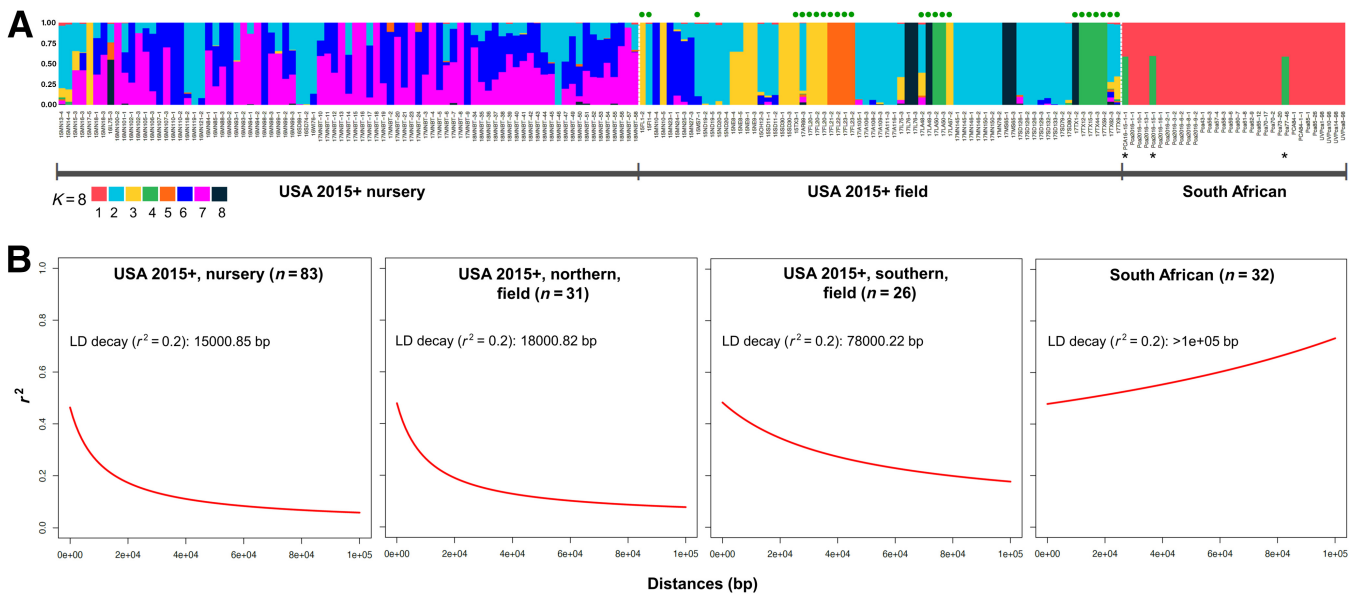


Fig. 3. Population structure analysis and linkage disequilibrium (LD) decay analysis of *Puccinia coronata* f. sp. *avenae* (*Pca*) isolates from the United States and South Africa. **A**, Population membership structure bar plot using 132,571 unlinked single-nucleotide polymorphisms (SNPs) and based on $K = 8$ clusters, the optimal number determined by cross-validation. Isolates labeled with green dots were collected from field oats in southern U.S. states where buckthorn is absent. No 1990 U.S. isolates were included. The three South African isolates marked with black asterisks originated from wild oats. Cluster identity is represented by colors shown in the key. **B**, LD decay plots based on 21,309 and 10,341 SNP variants identified against chromosome 1A of the *Pca*203 reference from U.S. isolates (excluding isolates from 1990) and South African isolates, respectively. Population subsets labeled for each plot with LD decay values indicated as a function of distance (bp) using $r^2 = 0.2$.

instance, isolates of phenotypic clusters 1 and 2 had highly similar virulence profiles but were clearly separated as genetically distinct groups by phylogeny. Likewise, eight isolates collected from the buckthorn nursery in 2017 had very similar pathotypes and clustered together phenotypically, but belonged to four genetically distinct clonal pairs that were widely separated in the phylogeny. These observations argue that race assignments are poor indicators of genetic relationships in rust populations with high levels of diversity.

In contrast, comparison of phenotypes of South African *Pca* isolates ($n = 32$) with a phylogenetic tree indicated a much clearer relationship, consistent with stepwise mutation of this single clonal lineage into groups with different pathotypes (Supplementary Fig. S8). Several mutation events can be placed onto the phylogenetic tree of this lineage, with branches showing co-mutation to virulence on multiple *Pc* genes. Branch A shows simultaneous mutation to virulence on *Pc39*, *Pc55*, and *Pc71*. Similarly, branch B shows mutation to virulence on *Pc48*, *Pc52*, and *Pc92*. Finally, branch C includes one or more mutations to virulence on eight *Pc* genes: *Pc39*, *Pc55*, *Pc71*, *Pc38*, *Pc57*, *Pc58*, *Pc59*, and *Pc63*.

Nuclear phased chromosome assembly enhances identification of virulence loci

To identify genomic regions linked to virulence on specific *Pc* genes, we conducted a GWAS analysis on isolates of the sexually recombining U.S. population. SNP genotypes were called separately against five reference assemblies: 12SD80 primary contigs; 12NC29 primary contigs; *Pca203* full-diploid genome; and the separate A and B haplotypes of *Pca203*. These datasets were analyzed for genetic associations with the virulence scores of these isolates on individual oat differential lines (Supplementary Data S2). In general, the use of the phased chromosome-scale *Pca203* reference resulted in better discrimination of association regions than the more fragmented 12SD80 and 12NC29 references (Fig. 4; Supplementary Data S2). For instance, association peaks that were split between multiple contigs in 12SD80 and 12NC29 were resolved to single peaks in the *Pca203* assembly for 16 oat lines (*Pc38*, *Pc39*, *Pc48*, *Pc51*, *Pc52*, *Pc53*, *Pc55*, *Pc57*, *Pc61*, *Pc91*, *Pc63*, *Pc68*, *Pc70*, *Pc71*, Belle, and HiFi). In contrast, for *Pc35*, *Pc58*, *Pc62*, and *Pc64*, single association peaks were detected on the 12SD80 and 12NC29 assemblies and were stronger than on *Pca203*. In all cases, contigs from

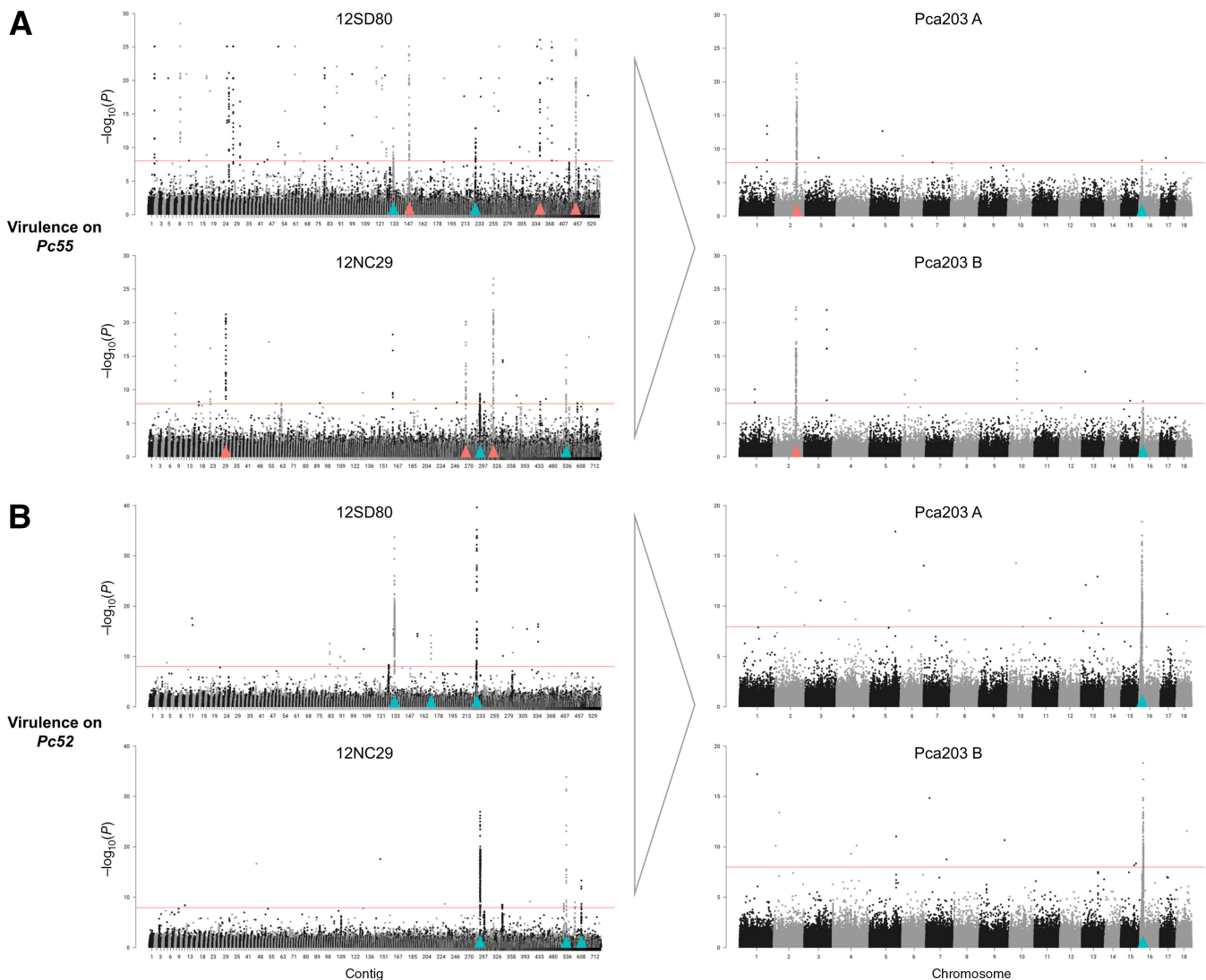


Fig. 4. Manhattan plots derived from genome-wide association study (GWAS) for virulence of U.S. isolates showing reduction in the number of association peaks using the fully phased *Pca203* reference (separate A and B haplotypes) compared with previous reference assemblies (12SD80, 12NC29). **A**, Association with virulence on *Pc55*. **B**, Association with virulence on *Pc52*. Bonferroni significance thresholds ($\alpha = 0.01/\text{total number of markers}$) are indicated by red horizontal lines. Peaks marked with red or teal arrows in 12SD80 or 12NC29 correspond to peaks marked with the same color in *Pca203* (A or B) based on sequence homology.

12SD80 and 12NC29 showing strong associations were syntenic with the chromosomal locations of the equivalent peaks in the *Pca203* genome (Supplementary Fig. S9; Supplementary Table S1). For oat lines H548 and Pc54, an association peak was detected only in 12SD80 and 12NC29 references, but no peak was detected in *Pca203* (Supplementary Data S2). Nonetheless, both 12SD80 and 12NC29 regions displayed synteny with each other and mapped to the same region on chromosome 1 of the *Pca203* reference.

In total, significant peaks of virulence-associated SNPs were detected for 25 of the 40 oat differentials. Many of these locations overlapped between different oat lines, giving a total of 11

significant VGIs (Table 1; Fig. 5). These VGIs span between 10 and 320 kbp on the *Pca203* genome. For 12 of the oat differential lines (TAM-O-405, Pc38, Pc39, Pc48, Pc51, Pc52, Pc55, Pc57, Pc61, Pc63, Pc70, and Pc71), the VGIs detected here correspond to those previously detected by Miller et al. (2020) using the 12SD80 and 12NC29 references and a smaller *Pca* population, although further refined here using the *Pca203* reference. Associations with the other 13 differentials were not previously detected, showing the value of the larger population size and chromosome-scale assembly. Only four VGIs were exclusive to a single oat line (VGI #5/Pc51, VGI #6/TAM-O-405, VGI #7/Pc53, and VGI #9/Belle), while the remainder were detected

Table 1. Virulence-associated genomic intervals (VGIs) determined from significant association peaks in both haplotypes (subgenomes) of *Pca203* along with counts of annotated genes and predicted effectors within VGIs

VGI #	Significant on <i>Pc</i> genes/oat lines ^a	Coordinates (length in kbp)		Total genes in VGI		Secreted of total		Effectors predicted of secreted	
		Hap A	Hap B	Hap A	Hap B	Hap A	Hap B	Hap A	Hap B
		1	Pc62, Pc64	chr1A: 2.14–2.20Mb (60)	chr1B: 1.98–2.02Mb (40)	8	5	0	1
2	Pc54, H548	chr1A: 4.01–4.03Mb (20)	chr1B: 3.76–3.77Mb (10)	4	3	1	0	1	0
3	Pc38, Pc39, Pc55, Pc63, Pc70, Pc71, WIX4361-9*, Pc57*, Pc61*, Pc91*	chr2A: 4.59–4.91Mb (320)	chr2B: 4.68–4.99Mb (310)	47	46	8	6	3	1
4	Pc57*, Pc61*	chr6A: 0.48–0.70Mb (220)	chr6B: 0.57–0.77Mb (200)	46	24	8	5	6	4
5	Pc51	chr6A: 2.74–2.84Mb (100)	chr6B: 2.86–2.93Mb (70)	9	7	1	1	1	0
6	TAM-O-405	chr10A: 4.60–4.71Mb (110)	chr10B: 4.70–4.80Mb (100)	29	12	5	2	1	0
7	Pc53*	chr11A: 3.21–3.24Mb (30)	chr11B: 3.12–3.14Mb (20)	11	7	1	0	0	0
8	Pc35, Pc58	chr11A: 5.35–5.38Mb (30)	chr11B: 5.08–5.11Mb (30)	5	6	1	1	1	0
9	Belle	chr13A: 2.97–3.25Mb (280)	chr13B: 2.35–2.53Mb (180)	39	35	1	1	0	0
10	Pc48, Pc52, HiFi*, TAM-O-405*, WIX4361-9*, Pc55*, Pc57*, Pc61*, Pc63*, Pc68*, Pc71*, Pc91*	chr16A: 0.44–0.75Mb (310)	chr16B: 0.56–0.77Mb (210)	32	29	3	1	2	1
11	Pc36*, Pc68, Pc91, HiFi	chr17A: 2.26–2.33Mb (70)	chr17B: 2.30–2.41Mb (110)	13	16	2	5	1	3
			Total	243	190	31	23	16	10

^a An asterisk (*) indicates minor association peak in these *Pc* genes/oat lines.

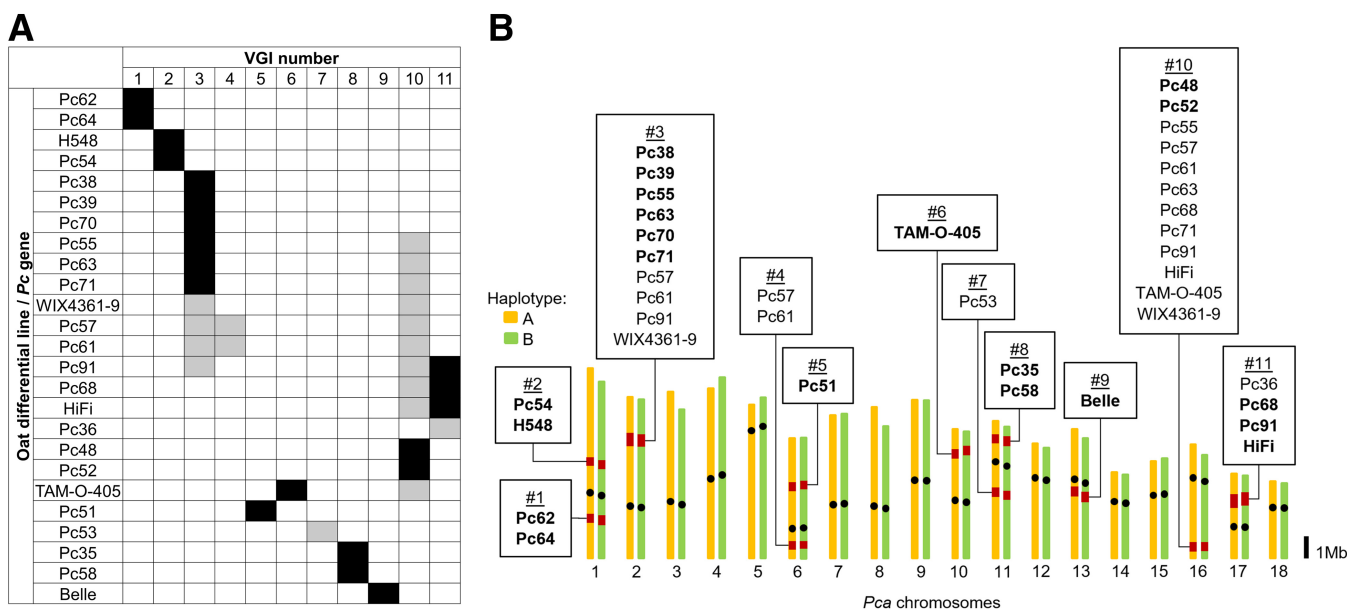


Fig. 5. Chromosomal map of *Pca203* showing locations of virulence associations. **A**, Matrix indicating presence of genome-wide association study (GWAS) peaks for virulence-associated genomic intervals (VGIs) in different oat differential lines. Black boxes denote presence of primary association peaks, and gray boxes denote presence of secondary or minor association peaks. *Pc* genes/oat lines are grouped by shared VGIs. **B**, Chromosomal map of *Pca203* showing locations of VGIs in red labeled with *Pc* genes/oat lines having significant associations. Bold text indicates *Pc* genes/oat lines producing a primary association peak on a given VGI, whereas normal text indicates those producing a secondary or minor association peak. Black dots denote approximate locations of centromeres.

by more than one oat differential line (Fig. 5). For example, four pairs of oat lines each detected a single strong association peak: Pc62 and Pc64 detecting VGI #1, Pc54 and H548 detecting VGI #2, Pc35 and Pc58 detecting VGI #8, and Pc48 and Pc52 detecting VGI #10. The latter, VGI #10, also appears as a minor peak for 10 other oat differential lines, while VGI #3 appears as a strong association peak for oat differential lines Pc38, Pc39, Pc70, Pc55, Pc63 and Pc71, and is also detected as a minor peak for Pc57, Pc61, Pc91 and WIX4361-9. Similarly, a common association on VGI #11 was detected for virulence on oat lines Pc36, Pc68, Pc91 and HiFi. Conversely, for 15 oat differential lines we detected a single VGI (Fig. 5; Supplementary Data S2), consistent with these lines containing a single effective *R* gene with a single corresponding *Avr* locus. However, the other 10 lines detected association peaks in two or more VGIs, suggesting that these oat differential lines may contain multiple different *R* genes.

Comparison of the resistance profiles of differential lines that detect the same VGIs showed substantial overlap in their recognition specificity, but also some differences (Fig. 6). For example, Pc35 and Pc58 both detected VGI #8 and showed similar profiles (Fig. 6A), although the Pc58 differential gave intermediate responses to isolates that were fully virulent on Pc35. Similarly, Pc48 and Pc52 (VGI #10) showed similar profiles, but with some isolates fully virulent on Pc52 giving intermediate responses on Pc48 (Fig. 6B). Similar observations were made for other lines detecting common VGIs (Fig. 6C to G). Overall,

these data suggest that *R* genes in some differential lines recognize *Avr* genes in *Pca* that occur at the same loci, either as allelic variants or closely linked genes.

To identify potential *Avr* gene candidates within the VGIs (Supplementary Data S1), we examined existing gene models (Henningesen et al. 2022) within each VGI (Table 1). All the VGIs contained at least one and up to eight gene models encoding secreted proteins in either haplotype, and between one and six of those were predicted as cytoplasmic or dual-localized effectors by EffectorP3.0 (Sperschneider and Dodds 2022), except in VGI #7 (Pc53) and VGI #9 (Belle), in which no effectors were predicted. VGI #3 corresponded to the highest number of virulence associations with oat differential lines, which included Pc38, Pc39, Pc55, Pc63, Pc70, and Pc71 and contained eight and six predicted secreted protein genes in the A and B haplotypes respectively, with three (A haplotype) and one (B haplotype) predicted as cytoplasmic effectors. The presence of multiple effector candidates in this region is consistent with the possibility that different oat *R* genes could recognize closely linked *Avrs*. On the other hand, VGI #10, which was also associated with virulence on a large number of differential lines, contained only one or two predicted effectors, suggesting that these differentials may recognize the same *Avr* gene, or alleles thereof.

To assess whether VGIs coincided with signals of recent host adaptation in *Pca*, we conducted a selective sweep analysis of the nursery isolates collected in 2015 onward (Supplementary Figs. S10 and S11). A total of 54 sweep loci were

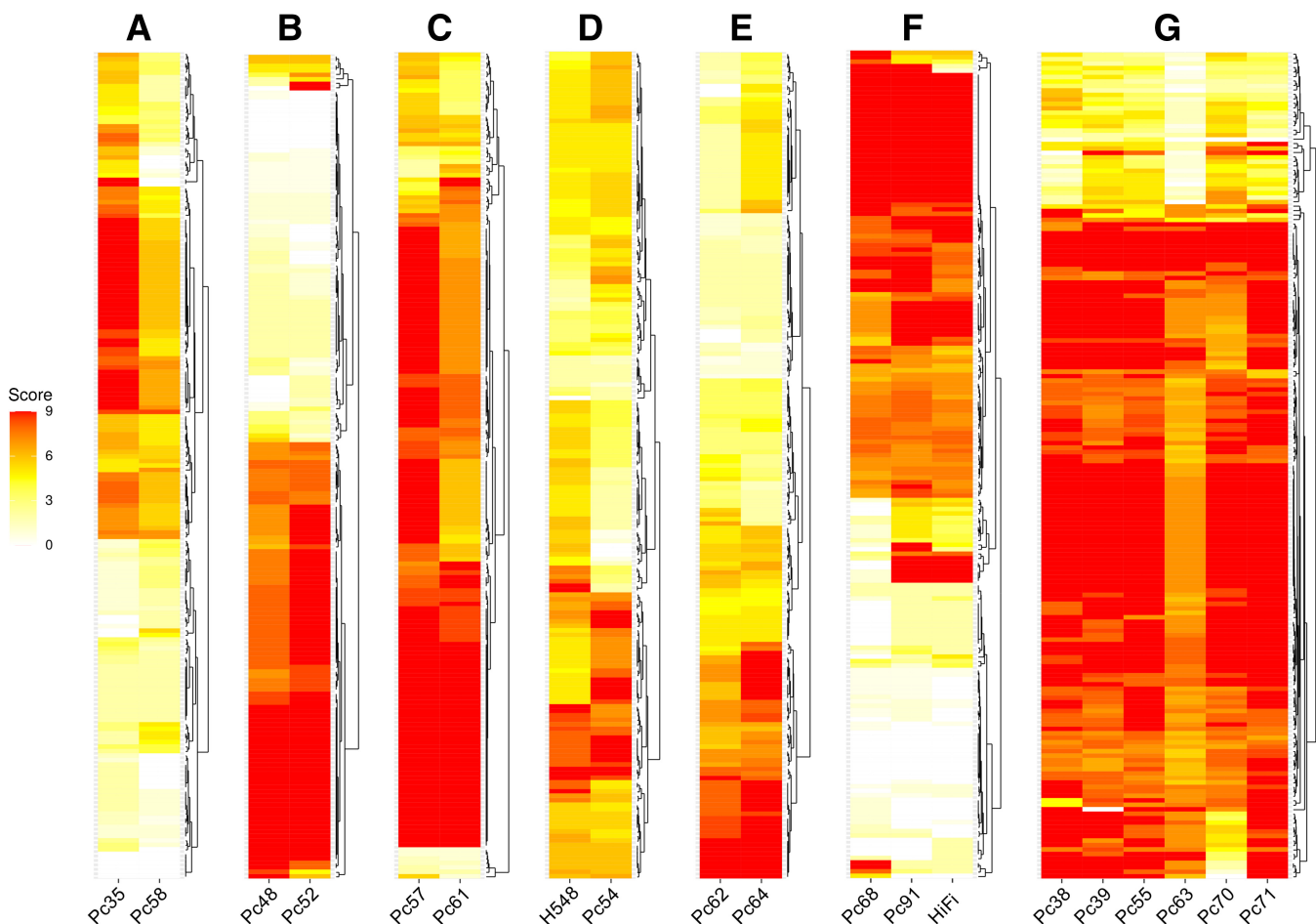


Fig. 6. Heat maps of virulence of 185 U.S. *Puccinia coronata* f. sp. *avenae* (*Pca*) isolates scored on oat differential lines grouped by shared genomic associations in *Pca*. High scores (red) indicate high virulence (disease susceptibility), and lower scores (yellow/white) indicate avirulence (disease resistance) on respective *Pc* genes/oat lines. Isolates of *Pca* (y axis) are ordered independently according to hierarchical clustering of scores. Oat lines (x axis) producing major virulence-associated genomic intervals (VGIs) in common are grouped accordingly: A, VGI #8; B, VGI #10; C, VGI #4; D, VGI #2; E, VGI #1; F, VGI #11; G, VGI #3.

identified, with 10 in the A haplotype and 44 in the B haplotype, ranging in size from 60 kbp to 183.5 kbp and spanning from 2 to 34 genes. Collectively, detected sweep loci summed to 611 kbp from the A subgenome and 3,186 kbp from the B subgenome. However, just 13 sweep loci on chr12B made up 1,247 kbp of this. Of all sweep loci detected, only two coincided with identified VGIs: VGI #3 on chromosome 2B associated with virulence on Pc38/39/55/63/70/71 and VGI #9 on chromosome 13A associated with virulence on Belle (Supplementary Fig. S11).

Discussion

Knowledge of pathogen population dynamics and the genetic architecture of host–pathogen interactions is important to understand the emergence of new virulence traits in response to the deployment of race-specific *R* genes in crops. The oat crown rust pathogen, *Pca*, has shown particularly rapid evolution of new virulence phenotypes in the United States, which is thought to be caused by the involvement of the alternate host, common buckthorn, allowing sexual reproduction and reassortment of virulence alleles. While investigating this hypothesis, Miller et al. (2020) found evidence for sexual recombination from genome sequence data of a limited sample of U.S. *Pca* isolates but also observed the accumulation of some clonal lineages. However, Miller et al. (2020) were not able to discriminate between different geographic regions in the United States where buckthorn is present or absent to establish a link between virulence evolution and sexuality. We took advantage of a new chromosomal-scale and nuclear phased reference genome of *Pca* (Henningsen et al. 2022) and a substantially larger collection of recent *Pca* isolates from the United States to expand on our understanding of the effects of geography and sexuality on the genetic diversity of *Pca*. We found that the *Pca* population in the northern United States, where buckthorn is prevalent, is almost entirely sexual in nature, as evidenced by the strong support for recombination in the neighbor-net tree, the extreme genetic separation of individual isolates in the phylogenetic tree, and the rapid decay of LD in this population. This suggests that the northern U.S. *Pca* population is mainly derived each growing season from sexually recombined aeciospores produced on buckthorn bushes during the previous winter. This contrasts with the situation observed in the United States for wheat and barley rust diseases, for which spore dispersal follows the well-known “*Puccinia* pathway” with infections manifesting from south to north as the season progresses and wind-borne inoculum from the earlier-planting southern regions spreading north as the season progresses (Fetch et al. 2011; Hamilton and Stakman 1967; Stakman and Harrar 1957). Initiation of these rust infections in northern regions are dependent on urediniospore inoculum spread from the south, as these pathogens cannot overwinter in the north because of the absence of a green bridge. However, the presence of the alternate host buckthorn allows *Pca* to overwinter in the north and initiate locally derived infections on oat at the start of the growing season through sexually derived aeciospores produced on buckthorn. This also underpins the high levels of genetic diversity in this population. *Pca* populations in the southern regions of the United States show more prevalent clonal lineages but nevertheless are still highly diverse and with low levels of LD. This indicates that southern populations are influenced by two separate factors—local propagation and maintenance of clonal lineages—as well as regular introductions of new sexually derived lineages by migration from the north. Survival of *Pca* lineages in the south could also be facilitated through infection of wild oats acting as an additional reservoir for the pathogen between growing seasons. Some genotypes detected in 2015 in the northern United States were found in southern areas in 2017, with some clonal

groups comprising both northern and southern isolates. Thus, north to south migration is also a significant factor in epidemiology of this disease, in addition to the traditional south to north *Puccinia* pathway. Consistent with this, annual race surveys in the United States have detected a sudden spread of virulence traits in the south in recent years that appeared to be preceded by a steady accumulation of virulence traits in the north (Moreau et al. 2024). Interestingly, our study also detected a long-lasting lineage still present in 2017 that has persisted in the United States since at least 1990 and includes isolates collected from both northern and southern states (Fig. 2, groups A and E). Our data also show evidence of increased virulence frequency on Pc68, Pc91, and HiFi oat differential lines between 2015 and 2017. This is consistent with a report from Canada (Menzies et al. 2019) showing that virulence on *Pc91* increased from 0% in 2011 to 66% by 2015, as well as more recent U.S. race surveys reporting up to 97% virulence on *Pc91* since 2020 from just 41% in 2015 (Moreau et al. 2024).

The South African *Pca* population (Boshoff et al. 2020) shows a sharp contrast with the U.S. population. South African isolates collected from cultivated oat across the country between 1998 and 2018 represent a single clonal lineage with genetic markers in complete LD. Interestingly, three isolates collected from wild oats in this region represented a different clonal lineage, although genetically related. A more in-depth sampling of the South African *Pca* population from wild oats will be required to determine the relationships between *Pca* on these different hosts. Unexpectedly, the U.S. isolate 90MN5B-1, collected in 1990, appears related to the South African *Pca* lineages. It is possible that 90MN5B-1 represents an exotic introduction with a founding effect in South Africa or that 90MN5B-1 and the South African population are commonly derived from a broader intercontinental lineage divergent from the U.S. population. Further studies on international collections of *Pca* will shed light on the distribution and diversity of different global lineages.

The use of a nuclear phased genome assembly for Pca203 and a larger population resulted in identification of virulence associations for more oat differential lines than was previously possible (Miller et al. 2020) and allowed for better resolution of VGIs in the *Pca* genome. However, the complementary use of the alternate references also aided in detecting associations that were significant in one reference but absent or weak in another; for instance, Pc54/H548 detected a strongly associated region on the 12SD80 and 12NC29 references, but not Pca203, although the latter reference helped to map this VGI to a chromosomal location. Such variation between references may result from divergence between the reference isolate and isolates from the analyzed populations, reducing the ability to map sequence reads and call SNPs in some regions. These biases may also emerge between haplotypes of the same reference isolate in genomic regions with sufficient divergence (Supplementary Data S2). Overall, we detected 11 VGIs in the *Pca* genome corresponding to 25 of the oat differential lines (Table 1; Fig. 5). In four cases, there were one-to-one relationships between single differential lines and VGIs: Pc51 (VGI#5), Pc57 (VGI#7), TAM-O-405 (VGI #6), and Belle (VGI #9), consistent with a simple gene-for-gene relationship between unique *R* and *Avr* gene pairs. In other cases, multiple oat lines detected the same VGI, such as Pc62 and Pc64 (VGI #1), Pc54 and H548 (VGI #2), Pc35 and Pc58 (VGI #8), and Pc48 and Pc52 (VGI #10). These may represent cases of the same *Pc* gene or an allelic variant recognizing the same *Avr* gene being independently incorporated into the oat differential set. In other cases, one *Pc* differential line detected multiple VGIs, suggesting the presence of multiple *R* genes in that one line. These complex situations urge careful evaluation of the composition of the oat differential set.

Although many of the differential lines have had very limited genetic analysis to determine the number or identity of *R* genes present, several reports in the oat crown rust pathosystem accompanied by virulence phenotypic comparisons can assist the interpretation of these GWAS results. For example, the Pc48 and Pc52 lines both detected the same *Pca* locus (VGI #10), which is consistent with the reported positive association for *Pc48* and *Pc52* virulence by Chong and Zegeye (2004). A single branch (B) in the South African clonal lineage showed mutation to virulence on both lines, supporting their recognition of the same *Avr* locus. However, although Pc48 and Pc52 (VGI #10) showed similar virulence profiles, they were differentiated by some isolates fully virulent on Pc52 that gave intermediate responses on Pc48 (Fig. 6B). This suggests they may carry related *R* genes or alleles of the same *R* gene that recognize the same *Avr* effector but with some quantitative differences in recognition. Similarly, Pc35 and Pc58 both detected VGI #8 and showed similar resistance profiles (Fig. 6A), although the Pc58 differential gave intermediate responses to isolates that were fully virulent on Pc35. Mapping studies have also suggested *Pc58* resistance is conditioned by a cluster of three genes (Hoffman et al. 2006), supporting a possible distinction from *Pc35*. The genes *Pc39*, *Pc55*, and *Pc71* were shown to be closely linked and postulated as either allelic or identical (Kiehn et al. 1976; Leonard et al. 2005). This is consistent with the observation that they all detect VGI #3 in the GWAS. Furthermore, we observed a single branch (A) in the South African *Pca* clonal lineage with mutation to virulence on these three genes, consistent with these genes recognizing the same *Avr* gene and virulence arising from a single mutational event. Similarly, Harder et al. (1980) proposed genetic linkage or allelism of *Pc38* and *Pc63*, which also detect VGI #3. However, the South African mutant branch A clearly differentiates Pc38 and Pc63 from Pc39, Pc55, and Pc71, despite branch C appearing to show simultaneous mutation to virulence on all these lines. Additionally, individual mapping studies have assigned *Pc38*, *Pc71*, and *Pc39* to different locations in the oat linkage map (Bush and Wise 1998; Sowa and Paczos-Grzęda 2020; Wight et al. 2005). Given the complex rearrangements seen in the oat genome references, this may reflect the translocation of syntenic regions to different genomic positions through independent introgressions. Thus, these *Pc* genes may detect separate but closely linked *Avr* loci or potentially have varied recognition of allelic variants of the same *Avr* gene.

Several oat differential lines detected virulence associations at multiple VGIs, suggesting they may contain multiple *R* genes. For instance, the cultivar WIX4361-9 was reported to carry two unspecified *Pc* genes (Bonnett 1996) and detected VGI #3 and VGI #10. Given that both VGI #3 and VGI #10 are also associated to virulence on multiple oat lines, the identity of those unknown *Pc* genes in WIX4361-9 remains unclear but could include variants of the Pc38/39/55/63/71 and Pc48/52 groups. Similarly, the *Pc91* oat differential detected three VGIs (#3, #10, and #11). Menzies et al. (2019) found a positive correlation of virulence to *Pc91* with both *Pc48* and *Pc39*, which is consistent with these latter two detecting VGI #3 and VGI #10, respectively, and may indicate the presence of three different *R* loci in this line. Given the high prevalence of virulence to the Pc48/52 and Pc38/39/55/63/71 groups in current populations of *Pca*, many isolates would not detect such background genes, explaining the original postulation of *Pc91*. The oat cultivar HiFi showed a very similar virulence profile to Pc91 and detected VGI #10 and VGI #11. HiFi was developed by a series of crosses including ‘Amagalon’, the differential line carrying *Pc91* (McMullen et al. 2005), so it is likely that it carries the same *Pc* gene(s). Pc68 also detected VGI #10 and VGI #11 and showed a similar resistance profile to Pc91 and HiFi, but these lines were distinguished by several isolates with reciprocal contrasting virulence

for *Pc68* and *Pc91*. Thus, these differentials may all contain multiple *R* genes with some of these shared between Pc68 and Pc91. This suggests that researchers independently identified and transferred alleles, or perhaps the same variant, from wild relatives *Avena sterilis* and *Avena magna*, calling them *Pc68* and *Pc91*, respectively (Rooney et al. 1994; Wong et al. 1983).

The complex virulence relationships on some oat lines involving multiple loci with overlapping associations highlight limitations in our knowledge of the genetics of resistance in some of these differentials and the molecular basis of recognition. Other than the presence of multiple genes in some differentials, as described earlier, other explanations for this complexity include epistatic interactions between virulence loci and the presence of multiple *Avr* genes in a genetic cluster. For example, two *Avr* genes are separated by only 15 kbp in the genome of wheat stem rust, yet are specific to unrelated *R* genes (*Sr35* and *Sr50*) (Li et al. 2019). Conversely, the wheat powdery mildew *R* gene *Pm1* was found to detect two separate, unlinked *Avr* loci, each encoding proteins predicted to have structural similarity (Kloppe et al. 2023). Epistasis may also present as alternative pathogen loci that moderate the virulence response, such as inhibitor loci that suppress recognition of certain *Avr* genes, as observed in flax rust (Jones 1988) and wheat powdery mildew (Bourras et al. 2015).

Here, we established the role of geography, sexuality, and clonality as factors shaping the virulence evolution of *Pca*. Future exploration on the influence of wild oat populations is also warranted. Nevertheless, the possible contribution of somatic hybridization to the genetic diversity and evolutionary capacity of the pathogen cannot be ruled out until additional haplotype genome references are available. Ongoing work to generate a pangenome of *Pca* and capture haplotype diversity across geographic regions and clonal lineages will help to investigate this possibility and will likely improve the capacity of GWAS to identify *Avr* loci and isolate candidate genes. Rust population surveillance has relied heavily on the characterization of virulence profiles and subsequent race (pathotypes) assignment to infer genetic relationships among rust isolates and populations. While such practices can be informative in a wholly clonal population carrying lineage-specific mutations (e.g., South African subpopulations), the occurrence of incursions, sexual recombination, and somatic hybridization and the presence of multiple *Avr* loci can confound associations between phylogeny and race assignment caused by shuffling of virulence alleles. The integration of phenotypic data with high-resolution genotypic data from key rust lineages and haplotype combinations will transform rust surveillance programs by bringing speed, depth, and consistency to surveys around the globe. In the meantime, it would be beneficial to invest in a thoroughly characterized and curated differential set of nonredundant isogenic lines. For this, additional efforts to genetically map *Pc* genes as well as develop and implement high-quality molecular markers would be instrumental, not only for robust pathotyping, but also to screen and identify novel sources of oat crown rust disease resistance.

Materials and Methods

Rust sampling, plant inoculations, and virulence phenotyping and comparisons

P. coronata f. sp. *avenae* (*Pca*) isolates from the annual surveys by the USDA-ARS Cereal Disease Laboratory (St. Paul, MN, U.S.A.) were accessed as single-pustule cultures either from -80°C storage or through the oat-cropping season. Isolates were subjected to a second single-pustule purification and increased and tested for purity (Miller et al. 2018). Forty-six isolates were collected from aecia on buckthorn leaves at the Minnesota Matt Moore Buckthorn Nursery (St. Paul, MN, U.S.A.) (Supplementary Data S1) and inoculated onto oat cultivar

'Marvelous' for a two-step single-pustule purification followed by spore increase. Thirty-two *Pca* isolates were collected in South Africa in 1998, 2005, 2016, 2017, and 2018, including three isolates from wild oats (Boshoff et al. 2020), and were increased from single pustules on the oat cultivar 'Makuru'. The virulence pathotypes for U.S. isolates were defined using a set of 40 North American oat differential lines (Nazareno et al. 2018), while South African pathotypes were defined on a smaller differential set with some common lines (Boshoff et al. 2020). Infection types were scored 10 to 12 days after inoculation, with a scale of "0", "0;", ":", ":", "C", "1;", "1", "2", "3", "3+", and "4" (Miller et al. 2020) which was converted to a 0 to 9 numeric scale, and mean values from two independent score readings were used for statistical analysis. Race assignments were made according to standard 4-letter and 10-letter letter nomenclatures (Chong et al. 2000; Nazareno et al. 2018).

Wilcoxon rank sum tests were performed as two-tailed operations using the *wilcox.test* function in RStudio (v4.0.2; RStudio-Team 2022) to compare overall virulence between isolate groups using pooled scores from the entire oat differential set as well as that of individual differential lines. Violin plots of overall virulence distribution along with box plots of gene-specific virulence distribution between isolate groups were generated using ggplot2 (v3.3.6; Wickham 2016). Clustered heat maps were made from the scoring matrices using the R package ComplexHeatmap (v1.14.0; Gu et al. 2016).

For geographic comparisons, northern U.S. states with buckthorn prevalent were considered to be Minnesota (MN), Wisconsin (WI), North Dakota (ND), Nebraska (NE), Iowa (IA), Illinois (IL), and Pennsylvania (PA), while southern states where buckthorn is rare or absent were Kansas (KS), Arkansas (AR), Texas (TX), Louisiana (LA), Missouri (MS), Georgia (GA), and Florida (FL). Isolates from South Dakota (SD) ($n = 12$) were excluded from this analysis, because this state is geographically northern but has a low prevalence of buckthorn Rawlins et al. (2018).

DNA sequencing, read mapping, and variant calling

DNA was extracted from 20 mg of urediniospores of each isolate with the G-Biosciences Omniprep DNA isolation kit, and the Illumina TruSeq Nano DNA library preparation protocol was used for sequencing with Illumina NovaSeq on an S2 flow cell to generate 150-bp paired-end reads as described in Henningsen et al. (2022). FASTQ reads were trimmed with Trimmomatic (v0.38; Bolger et al. 2014) with a sliding window of 15 bp (incremented by 4 bp), leading and trailing low-quality (<10) bases removed, adapter clipping (seed mismatches set to 2, palindrome threshold of 30, simple clip threshold of 10, minimum adapter length of 2), and reads less than 100 bp discarded. Trimmed reads were aligned independently to the reference genomes (12SD80 and 12NC29 primary contigs, Pca203 A subgenome, Pca203 B subgenome, and Pca203 full-diploid set) using the *bwa mem* algorithm of BWA (v0.7.71; Li and Durbin 2009). BAM files were processed with SAMtools (v1.12; Li et al. 2009) and Picard (v2.26.9; <https://broadinstitute.github.io/picard>), including removal of duplicate reads and relabeling of reads by sample. Coverage statistics were generated using 'samtools depth -a' and piped to a custom AWK script, then plotted using R (<https://github.com/TC-Hewitt/OatCrownRust>).

Variant calling was performed separately for each reference using FreeBayes (v1.3.5; Garrison and Marth 2012) with option '--use-best-n-alleles 6', and VCF files were filtered using *vcffilter* of *vcflib* (v1.0.1; <https://github.com/vcflib/vcflib>) with the parameters 'QUAL > 20 & QUAL/AO > 10 & SAF > 0 & SAR > 0 & RPR > 1 & RPL > 1 & AC > 0.' VCFtools (v0.1.16; Danecek et al. 2011) was then used to select biallelic sites with less than 10% missing data

and minor allelic frequency of 5% or greater. Allele balance plots were generated from SNPs called against 12NC29 using a custom R script (https://github.com/henni164/Pca203_assembly/blob/master/figure_s2/203_frequencies.R). Genome assemblies and accompanying annotations of 12SD29 and 12NC80 were sourced from the DOE-JGI MycoCosm Portal (http://genome.jgi.doe.gov/PuccoNC29_1; http://genome.jgi.doe.gov/PuccoSD80_1).

Phylogenetic analysis

VCF output was converted to NEXUS and PHYLIP formats with *vcf2phylib* (<https://github.com/edgardomortiz/vcf2phylib>). Phylogenetic analysis was performed in RAXML (v8.2.12; Stamatakis 2014) using SNPs called in 12SD80 using PHYLIP input with ML criterion, 500 bootstrap replicates, and a general time-reversible CAT model. Trees were visualized in iTOL (v5; Letunic and Bork 2021).

For phylogenetic analysis of only South African isolates, a subset was taken from the raw VCF of variant calls against 12SD80, with filtering and selection performed as described in the above section. Analysis was performed using RAXML as above, except with 1,000 bootstrap replicates. The R package *ggtree* (v3.4.0; Yu et al. 2017) was used to illustrate the phylogenetic tree and virulence heat map using the *heatmap* function. Likewise, phylogenetic analysis of 65 clonal isolates from the U.S. population were taken as a subset from the original VCF file and processed as described above. The phylogenetic tree was created with *ggtree* as above, while the cluster dendrogram was generated using the R package *ggdendro* (v0.1.23; <https://github.com/andrie/ggdendro>). Accompanying virulence heat maps ordered by cluster or by phylogeny were generated separately using *ggplot2* (v3.3.6). An unrooted phylogenetic network was created from the NEXUS file, and PHI tests (Bruen et al. 2006) for signatures of past recombination were performed using *SplitsTree* (v4.16.2; Huson and Bryant 2006).

Population structure, linkage disequilibrium, and selective sweep analysis

Reference 12SD80 was considered optimal for population-based analyses (including phylogeny) because it more closely represented modern *Pca* populations, allowing detection of the most SNPs, whereas the higher contiguity of reference Pca203 was optimal for distance measurements and defining loci. Isolates from 1990 were excluded from membership, LD, and selective sweep analyses to eliminate biases due to temporal variation. Population structure was investigated using a model-based approach implemented using fastSTRUCTURE (Raj et al. 2014) on SNPs called against 12SD80. SNP pairs were pruned, maintaining only markers with $r^2 < 0.6$ in 500-kbp windows, using '+prune' in BCFtools (v1.15.1) (Danecek et al. 2021). Elbow plots were generated using the script 'chooseK.py' from fastSTRUCTURE and membership assignment bar plots generated using the R package *pophelper* (v1.2.0) and the program CLUMPP (v1.1.2) (Jakobsson and Rosenberg 2007; Francis 2017). Principal component analysis was performed on pruned SNPs using the '--pca' function in PLINK v2.0 (Chang et al. 2015) and plots generated in RStudio (v4.0.2) using *ggplot2* (v3.3.6). LD decay was estimated using SNPs called against chromosome 1 A of Pca203 in windows of 100 kb using the function '--geno-r2' and option '--ld-window-bp 100000' in VCFtools.

Selective sweeps were identified based on SNPs called against the Pca203 full-diploid reference using a composite likelihood ratio (CLR) method implemented in SweeD (v3.0; Pavlidis et al. 2013). Only isolates sampled from the buckthorn nursery were included based on membership analysis using $K = 5$ and a

membership value above 0.9 for cluster 1 (Supplementary Fig. S10). Isolates assigned to a different genetic cluster by fastSTRUCTURE were removed, resulting in a final dataset of 41 isolates. SweeD was run against individual chromosomes using the option “-folded” in 1-kb grids with significance threshold set at the 999th percentile. SNP density was determined across the genome in non-overlapping windows of 50 kbp, and only CLR values within 50-kbp regions with at least 35 SNPs were kept. Karyoplots illustrating chromosomal positions of VGIs and selective sweep loci were created using the R package karyoploteR (Gel and Serra 2017) with manually generated GRanges input.

GWAS

Virulence association testing was performed using 182 U.S. *Pca* isolates (Supplementary Data S1) based on scored phenotypes (0- to 9-point scale) for each oat differential line. Filtered biallelic SNPs were called for this dataset against primary contigs of 12SD80 (1,012,613 sites) and 12NC29 (856,274 sites), and chromosomes of *Pca203* diploid (372,275 sites) and A and B haploid (937,120 and 956,257 sites) genome references, as described above. Marker-trait associations were conducted for virulence scores on each of the 40 oat differential lines in TASSEL (v5.2.63; Bradbury et al. 2007) using a mixed linear model, with population structure and kinship calculated using four principal components and centered identity by state, respectively. No compression was performed, and variance components were re-estimated after each marker. Quantile–quantile and Manhattan plots were generated in R using the qqman package (v0.1.8; Turner 2018). The R package RAINBOWR (Hamazaki and Iwata 2020) was used to compute false discovery rates (FDR) at 5%. Bonferroni correction thresholds were calculated by dividing the *P* value of 0.01 (or 0.05 for the *Pca203* diploid genome) by the number of markers in each reference. This resulted in a threshold of 9.875×10^{-9} for 12SD80, 1.168×10^{-8} for 12NC29, 1.0671×10^{-8} for *Pca203* A subgenome, and 1.0457×10^{-8} for *Pca203* B subgenome. For the *Pca203* diploid genome, which had fewer markers, an $\alpha = 0.05$ was used, resulting in a threshold of 1.3431×10^{-7} .

VGIs were determined from separate analyses on A and B subgenomes of *Pca203* and were defined based on the start and end positions of the set of SNP markers within an association peak that exceeded the Bonferroni significance threshold, expanded to the nearest kilobase. For associations with few markers above the Bonferroni threshold, the FDR threshold was used instead (VGI #1, VGI #7, VGI #8, and VGI #9).

Synten analysis and effector prediction

To check for synteny between virulence-associated regions of the three genome references, alignments were visualized using D-Genies (Cabanettes and Klopp 2018). Whole-genome alignment of 12SD80 and 12NC29 haplotigs to *Pca203* chromosomes was performed using minimap2 (v2.24; Li 2018). SAMtools (v1.12) was used for extraction of significant regions and haplotigs from reference FASTAs, and minimap2 was again used for all-versus-all alignments of extracted sequences using option “-X” to avoid self-hits. Synteny plots were generated using the R package gggenomes (Hackl and Ankenbrand 2022) in RStudio (v4.0.2). Protein sequences were compared using BLAST+ (v2.13.0; Camacho et al. 2009) and ClustalOmega (Sievers and Higgins 2018). Secreted proteins were predicted using SignalP (v4.1; Petersen et al. 2011) (-t euk -u 0.34 -U 0.34) and TMHMM (v2.0; Krogh et al. 2001). A fungal protein was considered secreted if it was predicted to have a signal peptide and had no transmembrane domains outside the N-terminal region. Effector proteins were predicted with EffectorP (v3.0; Sperschneider and Dodds 2022).

Data Availability

Raw Illumina sequence reads of 162 U.S. and South African isolates used in this study are available in the NCBI BioProject PRJNA660269. Reads of 62 U.S. isolates used in this study generated by Miller et al. (2020) are available in the NCBI BioProject PRJNA398546. Custom scripts and programs used for analysis in this publication are available at <https://github.com/TC-Hewitt/OatCrownRust>. VCF files for future marker assisted diagnosis used in this study are available at the CSIRO Data Portal <https://data.csiro.au/collection/csiro:60078>. *Pca203* assembly and RNA sequencing reads (Henningesen et al. 2022) used in this study are available at <https://doi.org/10.25919/fdb7-sc82>.

Acknowledgments

Thanks to Alex Whan and Shannon Dillon at CSIRO for helpful discussions regarding GWAS and to Jakob Riddle and Roger Caspers at the USDA-ARS for assistance with race assignments.

Literature Cited

- Arndell, T., Chen, J., Sperschneider, J., Upadhyaya, N. M., Blundell, C., Niesner, N., Wang, A., Swain, S., Luo, M., Ayliffe, M. A., Figueroa, M., Vanhercke, T., and Dodds, P. N. 2023. Pooled effector library screening in protoplasts rapidly identifies novel *Avr* genes. *bioRxiv* 538616.
- Bolger, A. M., Lohse, M., and Usadel, B. 2014. Trimmomatic: A flexible trimmer for Illumina sequence data. *Bioinformatics* 30:2114-2120.
- Bolton, M. D., Kolmer, J. A., and Garvin, D. F. 2008. Wheat leaf rust caused by *Puccinia triticina*. *Mol. Plant Pathol.* 9:563-575.
- Bonnett, D. G. 1996. Host: pathogen studies of oat leaf rust in Australia. PhD thesis. University of Sydney, Australia.
- Boshoff, W. H. P., Pretorius, Z. A., Terefe, T., and Visser, B. 2020. Occurrence and pathogenicity of *Puccinia coronata* var *avenae* f. sp. *avenae* on oat in South Africa. *Crop Prot.* 133:105144.
- Bourras, S., McNally, K. E., Ben-David, R., Parlange, F., Roffler, S., Praz, C. R., Oberhaensli, S., Menardo, F., Stirnweis, D., Frenkel, Z., Schaefer, L. K., Flückiger, S., Treier, G., Herren, G., Korol, A. B., Wicker, T., and Keller, B. 2015. Multiple avirulence loci and allele-specific effector recognition control the *Pm3* race-specific resistance of wheat to powdery mildew. *Plant Cell* 27:2991-3012.
- Bradbury, P. J., Zhang, Z., Kroon, D. E., Casstevens, T. M., Ramdoss, Y., and Buckler, E. S. 2007. TASSEL: Software for association mapping of complex traits in diverse samples. *Bioinformatics* 23:2633-2635.
- Bruen, T. C., Philippe, H., and Bryant, D. 2006. A simple and robust statistical test for detecting the presence of recombination. *Genetics* 172:2665-2681.
- Bush, A. L., and Wise, R. P. 1998. High-resolution mapping adjacent to the *Pc71* crown-rust resistance locus in hexaploid oat. *Mol. Breed.* 4:13-21.
- Cabanettes, F., and Klopp, C. 2018. D-GENIES: Dot plot large genomes in an interactive, efficient and simple way. *PeerJ* 6:e4958.
- Camacho, C., Coulouris, G., Avagyan, V., Ma, N., Papadopoulos, J., Bealer, K., and Madden, T. L. 2009. BLAST+: Architecture and applications. *BMC Bioinf.* 10:421.
- Carson, M. L. 2011. Virulence in oat crown rust (*Puccinia coronata* f. sp. *avenae*) in the United States from 2006 through 2009. *Plant Dis.* 95:1528-1534.
- Chang, C. C., Chow, C. C., Tellier, L. C., Vattikuti, S., Purcell, S. M., and Lee, J. J. 2015. Second-generation PLINK: Rising to the challenge of larger and richer datasets. *GigaScience* 4:s13742-015-0047-8.
- Chen, J., Upadhyaya, N. M., Ortiz, D., Sperschneider, J., Li, F., Bouton, C., Breen, S., Dong, C., Xu, B., Zhang, X., Mago, R., Newell, K., Xia, X., Bernoux, M., Taylor, J. M., Steffenson, B., Jin, Y., Zhang, P., Kanyuka, K., Figueroa, M., Ellis, J. G., Park, R. F., and Dodds, P. N. 2017. Loss of *AvrSr50* by somatic exchange in stem rust leads to virulence for *Sr50* resistance in wheat. *Science* 358:1607-1610.
- Chong, J., Leonard, K. J., and Salmeron, J. J. 2000. A North American system of nomenclature for *Puccinia coronata* f. sp. *avenae*. *Plant Dis.* 84:580-585.
- Chong, J., and Zegeye, T. 2004. Physiologic specialization of *Puccinia coronata* f. sp. *avenae*, the cause of oat crown rust, in Canada from 1999 to 2001. *Can. J. Plant Pathol.* 26:97-108.
- Danecek, P., Auton, A., Abecasis, G., Albers, C. A., Banks, E., DePristo, M. A., Handsaker, R. E., Lunter, G., Marth, G. T., Sherry, S. T., McVean, G., Durbin, R., and 1000 Genomes Project Analysis Group. 2011. The variant call format and VCFtools. *Bioinformatics* 27:2156-2158.

- Danecek, P., Bonfield, J. K., Liddle, J., Marshall, J., Ohan, V., Pollard, M. O., Whitwham, A., Keane, T., McCarthy, S. A., Davies, R. M., and Li, H. 2021. Twelve years of SAMtools and BCFTools. *GigaScience* 10:giab008.
- Dodds, P. N. 2023. From gene-for-gene to resistosomes: Flor's enduring legacy. *Mol. Plant-Microbe Interact.* 36:461-467.
- Dodds, P. N., and Rathjen, J. P. 2010. Plant immunity: Towards an integrated view of plant-pathogen interactions. *Nat. Rev. Genet.* 11:539-548.
- Duan, H., Jones, A. W., Hewitt, T., Mackenzie, A., Hu, Y., Sharp, A., Lewis, D., Mago, R., Upadhyaya, N. M., Rathjen, J. P., Stone, E. A., Schwessinger, B., Figueroa, M., Dodds, P. N., Periyannan, S., and Sperschneider, J. 2022. Physical separation of haplotypes in dikaryons allows benchmarking of phasing accuracy in Nanopore and HiFi assemblies with Hi-C data. *Genome Biol.* 23:84.
- Duplessis, S., Lorrain, C., Petre, B., Figueroa, M., Dodds, P. N., and Aime, M. C. 2021. Host adaptation and virulence in heteroecious rust fungi. *Annu. Rev. Phytopathol.* 59:403-422.
- Ellis, J. G., Lagudah, E. S., Spielmeier, W., and Dodds, P. N. 2014. The past, present and future of breeding rust resistant wheat. *Front. Plant Sci.* 5:641.
- Fetch, T., McCallum, B., Menzies, J., Rashid, K., and Tenuta, A. 2011. Rust diseases in Canada. *Prairie Soils Crops* 4:87-96.
- Figueroa, M., Dodds, P. N., and Henningsen, E. C. 2020. Evolution of virulence in rust fungi—Multiple solutions to one problem. *Curr. Opin. Plant Biol.* 56:20-27.
- Francis, R. M. 2017. pophelper: An R package and web app to analyse and visualize population structure. *Mol. Ecol. Resour.* 17:27-32.
- Gao, Y., Liu, Z., Farris, J. D., Richards, J., Brueggeman, R. S., Li, X., Oliver, R. P., McDonald, B. A., and Friesen, T. L. 2016. Validation of genome-wide association studies as a tool to identify virulence factors in *Parastagonospora nodorum*. *Phytopathology* 106:1177-1185.
- Garrison, E., and Marth, G. 2012. Haplotype-based variant detection from short-read sequencing. *arXiv 1207.3907v2 [q-bio.GN]*.
- Gel, B., and Serra, E. 2017. karyoploteR: An R/Bioconductor package to plot customizable genomes displaying arbitrary data. *Bioinformatics* 33:3088-3090.
- Gu, Z., Eils, R., and Schlesner, M. 2016. Complex heatmaps reveal patterns and correlations in multidimensional genomic data. *Bioinformatics* 32:2847-2849.
- Hackl, T., and Ankenbrand, M. 2022. gggenomes: A grammar of graphics for comparative genomics. R package version 0.9.9.9000. <https://github.com/thackl/gggenomes>
- Hamazaki, K., and Iwata, H. 2020. RAINBOW: Haplotype-based genome-wide association study using a novel SNP-set method. *PLoS Comput. Biol.* 16:e1007663.
- Hamilton, L. M., and Stakman, E. C. 1967. Time of stem rust appearance on wheat in the western Mississippi basin in relation to the development of epidemics from 1921 to 1962. *Phytopathology* 57:609-614.
- Harder, D. E., McKenzie, R. I. H., and Martens, J. W. 1980. Inheritance of crown rust resistance in three accessions of *Avena sterilis*. *Can. J. Genet. Cytol.* 22:27-33.
- Henningsen, E. C., Hewitt, T., Dugyala, S., Nazareno, E. S., Gilbert, E., Li, F., Kianian, S. F., Steffenson, B. J., Dodds, P. N., Sperschneider, J., and Figueroa, M. 2022. A chromosome-level, fully phased genome assembly of the oat crown rust fungus *Puccinia coronata* f. sp. *avenae*: A resource to enable comparative genomics in the cereal rusts. *G3* 12:jkac149.
- Hoffman, D. L., Chong, J., Jackson, E. W., and Obert, D. E. 2006. Characterization and mapping of a crown rust resistance gene complex (*Pc58*) in TAM O-301. *Crop Sci.* 46:2630-2635.
- Huson, D. H., and Bryant, D. 2006. Application of phylogenetic networks in evolutionary studies. *Mol. Biol. Evol.* 23:254-267.
- Jakobsson, M., and Rosenberg, N. A. 2007. CLUMPP: A cluster matching and permutation program for dealing with label switching and multimodality in analysis of population structure. *Bioinformatics* 23:1801-1806.
- Jones, D. A. 1988. Genetic properties of inhibitor genes in flax rust that alter avirulence to virulence on flax. *Phytopathology* 78:342-344.
- Kamal, N., Tsardakas Renhuldt, N., Bentzer, J., Gundlach, H., Haberger, G., Juhász, A., Lux, T., Bose, U., Tye-Din, J. A., Lang, D., van Gessel, N., Reski, R., Fu, Y.-B., Spégel, P., Ceplitis, A., Himmelbach, A., Waters, A. J., Bekele, W. A., Colgrave, M. L., Hansson, M., Stein, N., Mayer, K. F. X., Jellen, E. N., Maughan, P. J., Tinker, N. A., Mascher, M., Olsson, O., Spannagl, M., and Sirijovski, N. 2022. The mosaic oat genome gives insights into a uniquely healthy cereal crop. *Nature* 606:113-119.
- Kariyawasam, G. K., Richards, J. K., Wyatt, N. A., Running, K. L. D., Xu, S. S., Liu, Z., Borowicz, P., Farris, J. D., and Friesen, T. L. 2022. The *Parastagonospora nodorum* necrotrophic effector SnTox5 targets the wheat gene *Snn5* and facilitates entry into the leaf mesophyll. *New Phytol.* 233:409-426.
- Kiehn, F. A., McKenzie, R. I. H., and Harder, D. E. 1976. Inheritance of resistance to *Puccinia coronata avenae* and its association with seed characteristics in four accessions of *Avena sterilis*. *Can. J. Genet. Cytol.* 18:717-726.
- Kloppe, T., Whetten, R. B., Kim, S.-B., Powell, O. R., Lück, S., Douchkov, D., Whetten, R. W., Hulse-Kemp, A. M., Balint-Kurti, P., and Cowger, C. 2023. Two pathogen loci determine *Blumeria graminis* f. sp. *tritici* virulence to wheat resistance gene *Pm1a*. *New Phytol.* 238:1546-1561.
- Krogh, A., Larsson, B., von Heijne, G., and Sonnhammer, E. L. 2001. Predicting transmembrane protein topology with a hidden Markov model: Application to complete genomes. *J. Mol. Biol.* 305:567-580.
- Leonard, K. J., Anikster, Y., and Manisterski, J. 2005. Virulence associations in oat crown rust. *Phytopathology* 95:53-61.
- Letunic, I., and Bork, P. 2021. Interactive Tree Of Life (iTOL) v5: An online tool for phylogenetic tree display and annotation. *Nucleic Acids Res.* 49:W293-W296.
- Li, F., Upadhyaya, N. M., Sperschneider, J., Matny, O., Nguyen-Phuc, H., Mago, R., Raley, C., Miller, M. E., Silverstein, K. A. T., Henningsen, E., Hirsch, C. D., Visser, B., Pretorius, Z. A., Steffenson, B. J., Schwessinger, B., Dodds, P. N., and Figueroa, M. 2019. Emergence of the Ug99 lineage of the wheat stem rust pathogen through somatic hybridisation. *Nat. Commun.* 10:5068.
- Li, H. 2018. Minimap2: Pairwise alignment for nucleotide sequences. *Bioinformatics* 34:3094-3100.
- Li, H., and Durbin, R. 2009. Fast and accurate short read alignment with Burrows-Wheeler transform. *Bioinformatics* 25:1754-1760.
- Li, H., Handsaker, B., Wysoker, A., Fennell, T., Ruan, J., Homer, N., Marth, G., Abecasis, G., Durbin, R., and 1000 Genome Project Data Processing Subgroup. 2009. The Sequence Alignment/Map format and SAMtools. *Bioinformatics* 25:2078-2079.
- Martin, A., Moolhuijzen, P., Tao, Y., McLroy, J., Ellwood, S. R., Fowler, R. A., Platz, G. J., Kilian, A., and Snyman, L. 2020. Genomic regions associated with virulence in *Pyrenophora teres* f. *teres* identified by genome-wide association analysis and biparental mapping. *Phytopathology* 110:881-891.
- McMullen, M. S., Doehlert, D. C., and Miller, J. D. 2005. Registration of 'HiFi' Oat. *Crop Sci.* 45:1664.
- Menzies, J. G., Xue, A., Gruenke, J., Dueck, R., Deceuninck, S., and Chen, Y. 2019. Virulence of *Puccinia coronata* var *avenae* f. sp. *avenae* (oat crown rust) in Canada during 2010 to 2015. *Can. J. Plant Pathol.* 41:379-391.
- Miller, M. E., Nazareno, E. S., Rottschaefer, S. M., Riddle, J., Dos Santos Pereira, D., Li, F., Nguyen-Phuc, H., Henningsen, E. C., Persoons, A., Saunders, D. G. O., Stukenbrock, E., Dodds, P. N., Kianian, S. F., and Figueroa, M. 2020. Increased virulence of *Puccinia coronata* f. sp. *avenae* populations through allele frequency changes at multiple putative *Avr* loci. *PLoS Genet.* 16:e1009291.
- Miller, M. E., Zhang, Y., Omidvar, V., Sperschneider, J., Schwessinger, B., Raley, C., Palmer, J. M., Garnica, D., Upadhyaya, N., Rathjen, J., Taylor, J. M., Park, R. F., Dodds, P. N., Hirsch, C. D., Kianian, S. F., and Figueroa, M. 2018. *De novo* assembly and phasing of dikaryotic genomes from two isolates of *Puccinia coronata* f. sp. *avenae*, the causal agent of oat crown rust. *mBio* 9:e01650-17.
- Möller, M., and Stukenbrock, E. H. 2017. Evolution and genome architecture in fungal plant pathogens. *Nat. Rev. Microbiol.* 15:756-771.
- Moreau, E. L. P., Riddle, J. M., Nazareno, E. S., and Kianian, S. F. 2024. Three decades of rust surveys in the United States reveal drastic virulence changes in oat crown rust. *Plant Dis.* <https://doi.org/10.1094/PDIS-09-23-1956-RE>
- Nazareno, E. S., Li, F., Smith, M., Park, R. F., Kianian, S. F., and Figueroa, M. 2018. *Puccinia coronata* f. sp. *avenae*: A threat to global oat production. *Mol. Plant Pathol.* 19:1047-1060.
- Patpour, M., Hovmøller, M. S., Rodríguez-Algaba, J., Randazzo, B., Villegas, D., Shamanin, V. P., Berlin, A., Flath, K., Czembor, P., Hanzalova, A., Sliková, S., Skolotneva, E. S., Jin, Y., Szabo, L., Meyer, K. J. G., Valade, R., Thach, T., Hansen, J. G., and Justesen, A. F. 2022. Wheat stem rust back in Europe: Diversity, prevalence and impact on host resistance. *Front. Plant Sci.* 13:882440.
- Pavlidis, P., Živković, D., Stamatakis, A., and Alachiotis, N. 2013. SweeD: Likelihood-based detection of selective sweeps in thousands of genomes. *Mol. Biol. Evol.* 30:2224-2234.
- Peng, Y., Yan, H., Guo, L., Deng, C., Wang, C., Wang, Y., Kang, L., Zhou, P., Yu, K., Dong, X., Liu, X., Sun, Z., Peng, Y., Zhao, J., Deng, D., Xu, Y., Li, Y., Jiang, Q., Li, Y., Wei, L., Wang, J., Ma, J., Hao, M., Li, W., Kang, H., Peng, Z., Liu, D., Jia, J., Zheng, Y., Ma, T., Wei, Y., Lu, F., and Ren, C. 2022. Reference genome assemblies reveal the origin and evolution of allohexaploid oat. *Nat. Genet.* 54:1248-1258.

- PepsiCo. 2021. Avena sativa–OT3098 v2 hexaploid oat. <https://wheat.pw.usda.gov/jb?data=/ggds/oat-ot3098v2-pepsico>
- Petersen, T. N., Brunak, S., von Heijne, G., and Nielsen, H. 2011. SignalP 4.0: Discriminating signal peptides from transmembrane regions. *Nat. Methods* 8:785-786.
- Raj, A., Stephens, M., and Pritchard, J. K. 2014. fastSTRUCTURE: Variational inference of population structure in large SNP data sets. *Genetics* 197:573-589.
- Rawlins, K., Griffin, J., Moorhead, D., Barger, C., and Evans, C. 2018. EDD Maps—Early Detection & Distribution Mapping Systems. University of Georgia—Center for Invasive Species Ecosystem Health, Tifton, GA.
- Rooney, W. L., Rines, H. W., and Phillips, R. L. 1994. Identification of RFLP markers linked to crown rust resistance genes *Pc 91* and *Pc 92* in oat. *Crop Sci.* 34:940-944.
- RStudio Team. 2022. RStudio: Integrated Development Environment for R. RStudio, PBC, Boston, MA.
- Salcedo, A., Rutter, W., Wang, S., Akhunova, A., Bolus, S., Chao, S., Anderson, N., De Soto, M. F., Rouse, M., Szabo, L., Bowden, R. L., Dubcovsky, J., and Akhunov, E. 2017. Variation in the *AvrSr35* gene determines *Sr35* resistance against wheat stem rust race Ug99. *Science* 358:1604-1606.
- Saunders, D. G. O., Pretorius, Z. A., and Hovmøller, M. S. 2019. Tackling the re-emergence of wheat stem rust in western Europe. *Commun. Biol.* 2:51.
- Sievers, F., and Higgins, D. G. 2018. Clustal Omega for making accurate alignments of many protein sequences. *Protein Sci.* 27:135-145.
- Sowa, S., and Paczos-Grzęda, E. 2020. Identification of molecular markers for the *Pc39* gene conferring resistance to crown rust in oat. *Theor. Appl. Genet.* 133:1081-1094.
- Sperschneider, J., and Dodds, P. N. 2022. EffectorP 3.0: Prediction of apoplastic and cytoplasmic effectors in fungi and oomycetes. *Mol. Plant-Microbe Interact.* 35:146-156.
- Sperschneider, J., Hewitt, T., Lewis, D. C., Periyannan, S., Milgate, A. W., Hickey, L. T., Mago, R., Dodds, P. N., and Figueroa, M. 2022. Extensive somatic nuclear exchanges shape global populations of the wheat leaf rust pathogen *Puccinia triticina*. *bioRxiv* 518271.
- Stakman, E. C., and Harrar, J. G. 1957. Principles of Plant Pathology. Ronald Press, New York, NY.
- Stamatakis, A. 2014. RAxML version 8: A tool for phylogenetic analysis and post-analysis of large phylogenies. *Bioinformatics* 30:1312-1313.
- Turner, S. D. 2018. qqman: An R package for visualizing GWAS results using Q-Q and Manhattan plots. *J. Open Source Softw.* 3:731.
- Upadhyaya, N. M., Mago, R., Panwar, V., Hewitt, T., Luo, M., Chen, J., Sperschneider, J., Nguyen-Phuc, H., Wang, A., Ortiz, D., Hac, L., Bhatt, D., Li, F., Zhang, J., Ayliffe, M., Figueroa, M., Kanyuka, K., Ellis, J. G., and Dodds, P. N. 2021. Genomics accelerated isolation of a new stem rust avirulence gene-wheat resistance gene pair. *Nat. Plants* 7:1220-1228.
- Wickham, H. 2016. ggplot2: Elegant Graphics for Data Analysis. Springer-Verlag, New York, NY.
- Wight, C. P., O'Donoghue, L. S., Chong, J., Tinker, N. A., and Molnar, S. J. 2005. Discovery, localization, and sequence characterization of molecular markers for the crown rust resistance genes *Pc38*, *Pc39*, and *Pc48* in cultivated oat (*Avena sativa* L.). *Mol. Breed.* 14:349-361.
- Wong, L. S. L., McKenzie, R. I. H., Harder, D. E., and Martens, J. W. 1983. The inheritance of resistance to *Puccinia coronata* and of floret characters in *Avena sterilis*. *Can. J. Genet. Cytol.* 25:329-335.
- Yu, G., Smith, D. K., Zhu, H., Guan, Y., and Lam, T. T.-Y. 2017. ggtree: An R package for visualization and annotation of phylogenetic trees with their covariates and other associated data. *Methods Ecol. Evol.* 8:28-36.
- Zhong, Z., Marcel, T. C., Hartmann, F. E., Ma, X., Plissonneau, C., Zala, M., Ducasse, A., Confais, J., Compain, J., Lapalu, N., Amselem, J., McDonald, B. A., Croll, D., and Palma-Guerrero, J. 2017. A small secreted protein in *Zymoseptoria tritici* is responsible for avirulence on wheat cultivars carrying the *Stb6* resistance gene. *New Phytol.* 214: 619-631.